Chinese Chemical Letters 31 (2020) 239–243

Contents lists available at ScienceDirect

Chinese Chemical Letters

journal homepage: www.elsevier.com/locate/cclet

Communication

Graphene-supported biomimetic catalysts with synergistic effect of adsorption and degradation for efficient dye capture and removal

Qin Li[a], Xiaopei Wang[a], Xueqing Xiong[a], Shuihong Zhu[a], Zhaohui Meng[a], Yongying Hong[a], Changxu Lin[a], Xiangyang Liu[a,b,*], Youhui Lin[a,**]

[a] Research Institute for Biomimetics and Soft Matter, Department of Physics, Fujian Provincial Key Laboratory for Soft Functional Materials Research, Xiamen University, Xiamen 361005, China
[b] Department of Physics, National University of Singapore, Singapore 117542, Singapore

ARTICLE INFO

Article history:
Received 16 February 2019
Received in revised form 2 April 2019
Accepted 16 April 2019
Available online 18 April 2019

Keywords:
Nanozymes
Pollutant removal
Solid matrix
Supported catalyst
Synergistic effect

ABSTRACT

Design and development of iron porphyrin-based artificial enzymes system have been attracting a lot of attention. Herein, without any toxic reductant and harsh processing, we present a facile one-pot method to fabricate bifunctional catalytic nanocomposites consisting of graphene and hemin by using vitamin C as a mild reduction reagent. The presence of graphene helps the formation of a high degree of highly active and stable hemin on the graphene surface in a monomeric form through their $\pi-\pi$ stacking interaction. As a result, such nanocomposites possess a superior adsorption capacity and intrinsic peroxidase-like catalytic activity. Moreover, by the combination of their dye adsorption ability, RGO-hemin nanocomposites can serve as a suitable candidate for efficient capture and removal of dyes *via* a synergistic effect. Our findings may pave the way to apply graphene-supported artificial enzymes in a variety of fields, such as environmental chemistry, bionics, medicine, and biotechnology

The catalytic efficiency, mechanistic pathways, and structural complexity displayed by natural enzymes make them a tremendous source of inspiration for chemists and have fueled much research focused on mimicking the structural characteristics and the functions of enzymes [1]. Recently, due to the rapid growth in nanotechnology, many articles have been reported to design nano-sized artificial enzymes [2–5]. These studies could generally be divided into two categories: nanomaterials themselves with intrinsic enzyme-mimicking activities and nanomaterials as supports for fabricating high-performance artificial enzymes at the nanoscale. So far, many catalytically active nanomaterials have already developed into a new generation of enzyme mimics, such as magnetic nanoparticles (MNPs) [2,6,7], CeO_2 [8–11], V_2O_5 [12], AuNPs [13], NiO nanoparticles [14], carbon nanomaterials [15,16] and many hybrid composites [17,18]. On the other hand, attachment of functional building blocks (*e.g.*, metal complexes, porphyrins, and peptides) on nanomaterial-based supports can also give rise to the formation of nanoscale artificial enzymes [19]. Nanomaterials can provide excellent scaffolds for promoting biomimetic catalysis and a wide range of potential applications [20–22]. In comparison with natural enzymes, synthetic catalysts usually show advantages of low-cost, ease of preparation, and their sufficient stability against biodegradation and denaturation [2,4,15,19]. Notwithstanding all these advantages, their practical applications in native form are often hampered by several limitations. Most notably, such mimics usually possess the relatively low catalytic activity, which cannot match with the catalytic performance of enzymes.

Understanding the behavior of carbon nanomaterials in the biomimetic system has attracted a lot of attention in the recent past. Typically, graphene-based material, as an atomically thick sheet of sp^2-hybridized carbon atoms, is particularly impressive [4,21,22]. So far, the incorporation of graphene or its derivatives into traditional artificial enzymes provides a facile but highly effective way to tailor the activities and stabilities of catalysts. On the other hand, in modern society, a considerable amount of hazardous organic pollutants are being discharged into the environment along with the industrialization and urbanization resulting in negative impact on mankind and the ecological system [23–25]. Recently, our group reported a "green" decoration approach for the attachment of hemin on reduced graphene oxide (RGO) and applied this nanocomposite into efficient removal of dye

* Corresponding author at: Department of Physics, National University of Singapore, Singapore 117542, Singapore.
** Corresponding author.
E-mail addresses: liuxy@xmu.edu.cn (X. Liu), linyouhui@xmu.edu.cn (Y. Lin).

https://doi.org/10.1016/j.cclet.2019.04.039
1001-8417/

pollutants [22]. According to previous reports, hemin is easily assembled onto the surface of graphene *via* $\pi-\pi$ stacking interaction [20,21]. The graphene supported hemin can maintain monomeric hemin activity analogy to natural enzymes, which makes such system more active and stable in contrast to the free hemin [20,26]. However, abundant bovine serum albumin proteins adsorbed on RGO, which affects the accessibility of catalyst surface, and the nanocomposite becomes unstable under harsh conditions (*e.g.*, high temperature), which is mainly caused by protein denaturation. Herein, we present a green and facile strategy for preparation of hemin-graphene hybrid nanocomposites by utilizing vitamin C as a reductant, and demonstrate that the as-synthesized nanocomposites with adsorption and catalytic abilities can serve as robust catalysts for removal dyes.

Graphite powder was obtained from Alfa Aesar and used as received. Hemin, 3,3′,5,5′-tetramethylbenzidine (TMB), *o*-phenylenediamine (OPD), and di-azo-aminobenzene (DAB) were obtained from Sigma-Aldrich. Horseradish peroxidase (HRP, EC 1.11.1.7) was purchased from Sangon Biotech Co., Ltd. (Shanghai, China) and stored in a refrigerator at −20 °C. H_2O_2 (30%), terephthalic acid and sodium hydroxide were acquired from Beijing Chemicals (Beijing, China). Double distilled water (18.2 MΩ; Millipore Co., USA) was used throughout the work. The UV/visible spectra were recorded by a UV/vis/NIR Spectrometer (Lambda 750, PerkinElmer). Fluorescence measurements were carried out on an F97 fluorescence photometer (Lengguang Tech.). EDX analysis was carried out using Field-emission SEM (SU-70).

Graphene oxide (GO) was synthesized according to a modified Hummer's approach. Typically, 2.0 g graphite powder was dispersed in 46 mL concentrated H_2SO_4 under stirring in a 500 mL beaker at room temperature. Subsequently, 6 g $KMnO_4$ was slowly added into the mixture at 0 °C under stirring. After sonication for 10 h, 92 mL double distilled water was gradually added into the reaction system. After keep boiling for another 20 min, 280 mL double distilled water and 20 mL H_2O_2 (30%) were added. Finally, the as-prepared yellow supernatant was separated by centrifugation and washed with 5% HCl and double distilled water until the GO solution reached a neutral pH value.

A simple environment-friendly route was used to prepare graphene-hemin nanocomposites by using vitamin C as a reductant. Typically, 500 μL of 0.5 mmol/L hemin was dissolved in 10 mL of 0.01 mol/L NaOH aqueous solution, followed by the addition of 1 mL of 5 mg/mL GO and 5 mL of 20 mg/mL vitamin C by sonication for 30 min at room temperature. After further adjusting pH approximate to 12 by NaOH, the resulting suspension was incubated at 65 °C for overnight. The product was separated by centrifugation and washed with double distilled water several times.

Study of peroxidase-like catalytic activity: Typically, 0.5 mmol/L TMB and 100 mmol/L H_2O_2 were added to 1 mL RGO-hemin nanocomposites (5 μg/mL) in the 25 mmol/L citrate buffer (pH 4.0). A blue color product oxTMB could be produced with major absorbance peaks located at 370 nm and 652 nm.

Detection of hydroxyl radicals: In a typical procedure, 0.1 mL of 0.2 mg/mL graphene-hemin nanocomposites was added in 0.1 mL of 400 mmol/L H_2O_2 aqueous solution, followed by addition of 2 mL of 0.1 mmol/L terephthalic acid and 0.4 mmol/L NaOH. The mixture was centrifuged and then the fluorescence change of the supernatant was monitored by fluorescence spectrophotometer at the excitation wavelength of 312 nm.

Electron paramagnetic resonance (EPR) detecteing the signals of radicals trapped by DMPO were recorded at ambient temperature using a Bruker EMX-10/12. In the experiments of hydroxyl radical formation, the sample inclued 50 μL 1 mg/mL RGO-hemin nanocomposites, 20 mmol/L DMPO, and 50 mmol/L H_2O_2 in 5 mmol/L phosphate buffer (pH 4).

The experiments of dye removal were carried out in 25 mmol/L phosphate buffer (pH 7.0). A series of different concentrations of graphene-hemin nanocomposites was added into 10 μg/mL MO or RB aqueous solution with or without H_2O_2 (100 mmol/L). All mixtures were kept at 30 °C for 3 h. After centrifugation, the obtained supernatant was measured by UV−vis spectrophotometer.

In recent decades, the design and development of iron porphyrin-based artificial enzymes system are particularly impressive [21,27,28]. Especially, hemin, the center for heme-proteins including peroxidases, hemoglobin, myoglobin, and cytochromes, can catalyze diverse oxidation reactions by itself similar to peroxidase enzymes. Its molecular structure is shown in Fig. S1 (Supporting information). However, even under physiological conditions, free hemin undergoes molecular aggregation and is easy to be oxidized and to cause its deactivation [21,28]. One of the most effective strategies is the incorporation of hemin onto solid matrices with a high specific surface area, such as graphene. Herein, the working principle for constructing RGO-hemin hybrid nanocomposites is schematically represented in Fig. 1A by simultaneous reduction of GO and attachment of hemin on the graphene surface. Briefly, 10 mL GO aqueous solution (0.5 mg/mL) obtained by a modified Hummer's approach, 1 mL hemin (0.01 mol/L) and 5 mL vitamin C (40 mg/mL) were firstly mixed and adjusted the pH of the mixture approximate to 12. Then, the resulting suspension was incubated at 65 °C for overnight. Finally, the as-prepared nanocomposites were purified by repeated centrifugation and washed with water. A control experiment showed that the original yellow-brown solution of GO transformed into the black after the reaction, and the resulting solution exhibited a strong peak at about 264 nm and its absorption intensity of the whole spectrum increased remarkably (Fig. 1B). These results indicated the successful reduction of GO to RGO by vitamin C and consequently the restoration of aromatic structure [20,22,29]. In this process, vitamin C was oxidized into dehydroascorbic acid (Fig. S3A in Supporting information) [30,31]. For

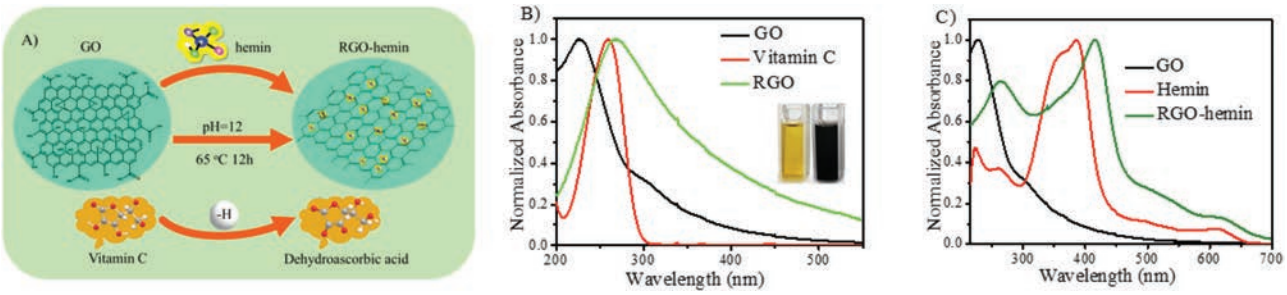

Fig. 1. (A) The working principle for one-pot facile fabrication of RGO-hemin nanocomposites by using vitamin C as a green reductant. (B) UV-vis spectra of GO, RGO and vitamin C. Insets show corresponding photographs of GO solution before and after reduction by vitamin C. (C) UV-vis spectra of GO, hemin and RGO-hemin.

the spectrum of free hemin solution, a strong peak at about 385 nm and an array weak peaks in 500-700 nm region were observed, which were attributed to the Soret band and Q-bands, respectively (Fig. 1C) [21,32]. After attachment of hemin on RGO, a large bathochromic shift for the Soret band of hemin was observed (Fig. 1C), implying the hemin molecules were anchored onto the RGO surface *via* π-π interaction successfully [21,32]. The hemin absorbed on the RGO was further confirmed by trace Fe element analysis in EDS (Fig. S2 in Supporting information).

To test the activity of as-prepared nanocomposites, one of typical peroxidase substrates 3,3′,5,5′-tetramethylbenzidine (TMB) was chosen (Fig. S3B in Supporting information). RGO-hemin nanocomposites could catalytically oxidize TMB in the presence of H_2O_2. After reaction, the color of the mixture changed from colorless to blue and the solution two adsorption peaks located at 370 nm and 652 nm were observed (Figs. 2A and B and Fig. S4 in Supporting information), demonstrating that the obtained RGO-hemin possesses peroxidase-like activity in the TMB oxidation reaction [2,4,6,19]. In contrast, the system containing RGO-hemin nanocomposites alone or only H_2O_2 did not show apparent oxidation toward TMB (Fig. 2A) and the catalytic activity of RGO-hemin nanocomposite was about 7 times higher than hemin alone (Fig. 2B). In addition, the peroxidase-like catalytic activity of RGO-hemin nanocomposites was also confirmed by choosing other peroxidase substrates, such as di-azo-aminobenzene (DAB) and *o*-phenylenediamine (OPD) (Fig. S4) Analogy to horseradish peroxidase (HRP), various colour products were formed towards representative peroxidase substrates, and the catalytic activity of as-obtained RGO-hemin nanocomposites also relied upon pH (Fig. S5 in Supporting information) [1,14,16,32]. In consideration of their robust stability, our synthetic nanomaterials are more suitable for practical application under relatively rigorous conditions than the natural enzyme HRP. According to previous reports, a common mechanism for the peroxidase-like activity of most peroxidase mimics is attributed to the decomposition of H_2O_2 to hydroxyl radicals (•OH) [33]. To investigate whether our catalytic activity was ascribed to the formation of •OH radicals, we selected terephthalic acid (TPA) as a probing molecule, which could produce a highly fluorescent product 2-hydro-terephthalic acid (HTPA) after reaction with hydroxyl radicals (Fig. S3B) [34,35]. In the presence of RGO-hemin nanocomposites and H_2O_2, the fluorescence peak intensity of TPA at 426 nm gradually increased during the catalytic process (Fig. 2C), which confirmed the catalytic activity of our nanocomposites was also attributed to the formation of •OH radicals. Furthermore, we adopted the electron paramagnetic resonance spectra (EPR) to convince the generation of •OH radicals using DMPO as the trapping agent [36,37]. As shown in Fig. 2D, the EPR spectra of RGO-hemin nanocomposites/H_2O_2 exhibited a typical 4-fold characteristic peak with an intensity ratio of 1:2:2:1. However, the EPR spectra of RGO-hemin alone did not show any obvious characteristic peak. These results indicated that •OH radicals were generated in RGO-hemin nanocomposites and H_2O_2 system.

Industrial wastewater is often polluted with synthetic dyes, there is an urgent need to degrade these refractory organics [38]. Previously, graphene and GO were researched as effective adsorbents toward anionic and cationic dyes [39]. When RGO-hemin nanocomposites used alone as an adsorbent, the RGO-hemin nanocomposites possessed relatively effective adsorption properties toward cationic dyes such as rhodamine B (RB) by observing the dramatic absorbance drop or the color change of supernatant after centrifugation of RGO-hemin nanocomposites, while had a poor effect toward anionic dyes such as methyl orange (MO) under the same condition (Fig. 3 and Fig. S6 in Supporting information). Note that RGO-hemin nanocomposites were removed to avoid background absorption interference before measurement. In addition, with increasing concentrations of RGO-hemin nanocomposites, the absorption spectrum of dyes gradually decreased (Figs. 3A and B), indicating a correlation between removal capacity and RGO-hemin nanocomposites dose. Control study showed that dyes themselves did not precipitate out under our experiment condition. By the combination of the negative nature of RGO-hemin nanocomposites at the neutral pH (Fig. S7 in Supporting information), we considered organic dyes were removed mainly through electrostatic adsorption between RGO-hemin nanocomposites and dyes.

After have demonstrated that our RGO-hemin nanocomposites themselves show certain removal capacity to dye pollutants and •OH radicals could be formed during the catalytic process, we then addressed the possibility of more efficiently scavenging dyes by our catalytically active nanomaterials *via* synergistic adsorption and degradation (Fig. 4). As demonstrated above, even for cationic dye RB, the high dose of RGO-hemin nanocomposites (60 μg/mL) needed for effectively scavenging dyes (Fig. 3E). However, in the presence of the low dose of RGO-hemin nanocomposites (10 μg/mL), without H_2O_2, the removal efficiency toward RB by adsorption was only about 40% after 3 h incubation (Fig. 3E). Using the same dose of RGO-hemin nanocomposites (10 μg/mL), more than 98% RB could be scavenged when 100 mmol/L H_2O_2 was used. Moreover, the adsorption of MO by RGO-hemin nanocomposites was almost negligible, while more than 92% of MO could be removed by the addition of 100 mmol/L H_2O_2. In addition, the removal of dyes increased with the increasing of RGO-hemin nanocomposites, indicated the degradation properties relied on the concentration of nano-catalysts (Fig. 4). Furthermore, with or without H_2O_2, the color change of the dyes-contained supernatant solutions could be easily distinguished by naked eyes after centrifugation of GO-hemin (Figs. 3C and D and Fig. S6). Based on the removal performance of RGO-hemin nanocomposites toward dyes in the absence and presence of H_2O_2, we inferred that the high performance of RGO-hemin/H_2O_2 system on dyes removal was owing to the combination of physical adsorption and chemical oxidation (Fig. 4A). The first step was to absorb dye compounds on the surface of RGO-hemin

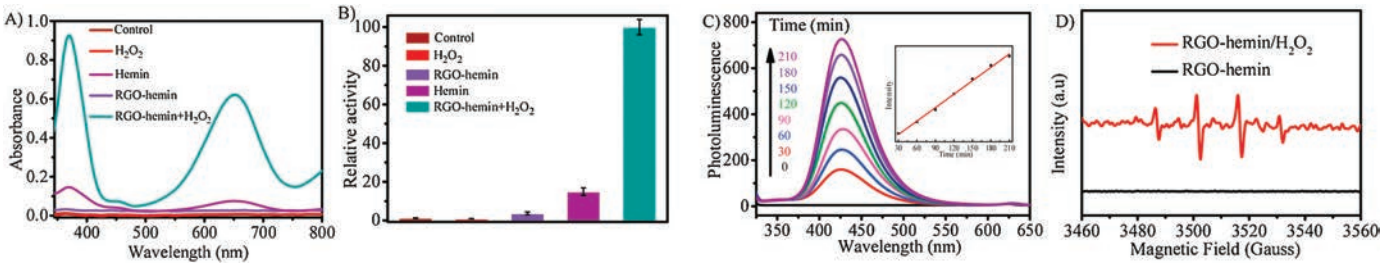

Fig. 2. (A) The absorption spectra of different samples in the presence of 1 mmol/L TMB after 10 min incubation. (B) The relative activity of different samples in the presence of 1 mmol/L TMB after 10 min incubation. (C) Time-dependent photoluminescence spectra of terephthalic acid by RGO-hemin nanocomposites and hydrogen peroxide. (D) DMPO trapped electron paramagnetic resonance spectra (EPR) at 120 s over RGO-hemin nanocomposites in the absence or presence of H_2O_2.

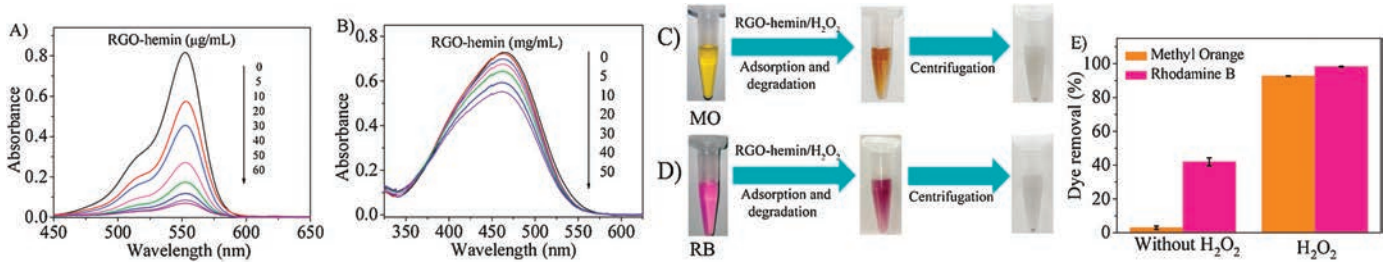

Fig. 3. (A, B) The adsorption capacity of diverse concentrations of RGO-hemin toward RB and MO at natural pH 7.0 after 3 h incubation. RGO-hemin nanocomposites were removed to avoid background absorption interference before measurement. (C, D) Visual color changes of MO and RB dyes before and after removal of dyes by RGO-hemin nanocomposites and hydrogen peroxide after 3 h incubation. (E) The dyes removal efficiency by RGO-hemin nanocomposites in the absence or presence of H_2O_2. The error bars represent the standard deviation of three parallel experiments. [RB] = 10 μg/mL, [MO] = 10 μg/mL, [RGO-hemin] = 10 μg/mL.

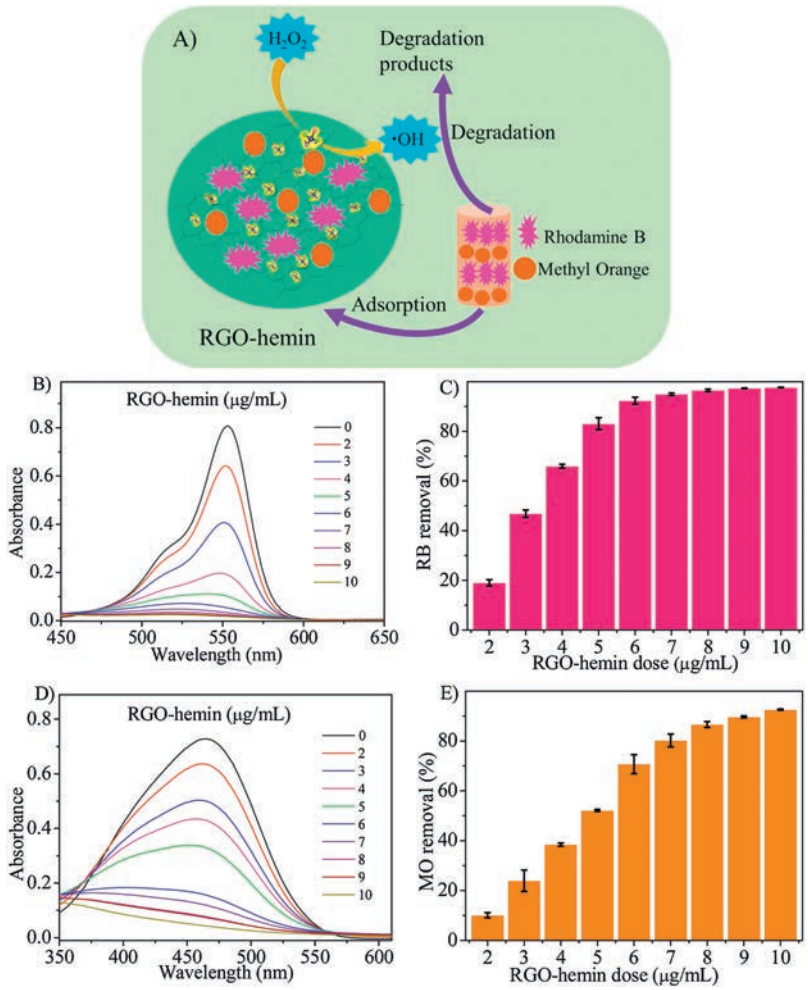

Fig. 4. (A) Schematic illustration of the high-performance removal of organic dyes by RGO-hemin nanocomposites for organic dyes *via* synergistic adsorption and degradation. The adsorption and degradation capacity of diverse concentrations of RGO-hemin toward (B, C) RB and (D, E) MO at natural pH 7.0 after 3 h incubation. RGO-hemin nanocomposites were removed to avoid background absorption interference before measurement. [RB] = 10 μg/mL, [MO] = 10 μg/mL, [H_2O_2] = 100 mmol/L.

nanocomposites. Due to such physical adsorption, dye compounds and the active sites of nanocomposites were anchored onto the same areas, which significantly improved the catalytic activity of our as-prepared nanocomposites [2,20,40,41]. Finally, RGO-hemin nanocomposites catalyzed H_2O_2 to the form of reactive $^{\bullet}OH$ radicals, and then consequently the degradation of dyes by produced $^{\bullet}OH$ radicals on the same nanoscale region. Our removal mechanism towards dye compounds is actually quite similar to that of natural enzymes, which possess excellent catalytic efficiency relying on their ability to bind substrates [20].

In conclusion, we have demonstrated an *in-situ*, green and facile strategy for fabrication of graphene-supported artificial enzymes in an aqueous solution by using vitamin C as a mild reductant, without toxic organic chemicals and harsh processing. The presence of graphene makes the supported hemin system more active and stable, in comparison with free hemin. The water-

soluble RGO-hemin nanocomposites could possess intrinsic peroxidase-like catalytic activity. Moreover, due to both adsorption and catalytic ability of as-prepared nanocomposites, they show excellent performance for removing no mater cationic or anionic dyes, such as MO and RB dyes under the natural pH, in the presence of H_2O_2. Our work may pave the way to use graphene as a scaffold for designing high-performance artificial enzymes and apply graphene-supported nano-catalysts in a variety of fields, such as environmental chemistry, bionics, medicine, and biotechnology.

Acknowledgments

This work was supported by the National Nature Science Foundation (Nos. 21771150, 21401154, U1405226), the Fundamental Research Funds for the Central Universities of China (Nos. 20720170011, 20720140528, 20720160127), 111 Project (No. B16029), and Doctoral Fund of the Ministry of Education (No. 20130121110018). Authors would like to acknowledge Dr. Hao Wang, Dr. Rui Yu and Dr. Yun Yang for their help with sample characterization.

Appendix A. Supplementary data

Supplementary data associated with this article can be found, in the online version, at https://doi.org/10.1016/j.cclet.2019.04.039.

References

[1] M. Stodulski, T. Gulder, Angew. Chem. Int. Ed. 51 (2012) 11202–11204.
[2] L. Gao, J. Zhuang, L. Nie, et al., Nat. Nanotechnol. 2 (2007) 577–583.
[3] J. Wu, X. Wang, Q. Wang, et al., Chem. Soc. Rev. 48 (2019) 1004–1076.
[4] Y. Lin, J. Ren, X. Qu, Acc. Chem. Res. 47 (2014) 1097–1105.
[5] W. Song, B. Zhao, C. Wang, et al., J. Mater. Chem. B 7 (2019) 850–875.
[6] J. Zhang, J. Zhuang, L. Gao, et al., Chemosphere 73 (2008) 1524–1528.
[7] K. Fan, C. Cao, Y. Pan, et al., Nat. Nanotechnol. 7 (2012) 459–464.
[8] A. Asati, C. Kaittanis, S. Santra, J.M. Perez, Anal. Chem. 83 (2011) 2547–2553.
[9] A. Asati, S. Santra, C. Kaittanis, et al., Angew. Chem. Int. Ed. 48 (2009) 2308–2312.
[10] B. Liu, Z. Huang, J. Liu, Nanoscale 8 (2016) 13562–13567.
[11] S.X. Zhang, S.F. Xue, J. Deng, et al., Biosens Bioelectron. 85 (2016) 457–463.
[12] F. Natalio, R. Andre, A.F. Hartog, et al., Nat. Nanotechnol. 7 (2012) 530–535.
[13] Y. Lin, J. Ren, X. Qu, Adv. Mater. 26 (2014) 4200–4217.
[14] D. Li, B. Liu, P.J. Huang, et al., Chem. Commun. 54 (2018) 12519–12522.
[15] K. Fan, J. Xi, L. Fan, et al., Nat. Commun. 9 (2018) 1440.
[16] Y. Song, K. Qu, C. Zhao, et al., Adv. Mater. 22 (2010) 2206–2210.
[17] Z. Wang, Y. Zhang, E. Ju, et al., Nat. Commun. 9 (2018) 3334.
[18] Y. Liu, Y.L. Qin, Y.L. Zheng, et al., J. Mater. Chem. B 7 (2019) 43–52.
[19] H. Wei, E. Wang, Chem. Soc. Rev. 42 (2013) 6060–6093.
[20] Y. Guo, L. Deng, J. Li, et al., Acs Nano 5 (2011) 1282–1290.
[21] T. Xue, S. Jiang, Y. Qu, et al., Angew. Chem. Int. Ed. 51 (2012) 3822–3825.
[22] X. Wang, C. Hou, W. Qiu, et al., ACS Appl. Mater. Interfaces 9 (2017) 684–692.
[23] Z. Aksu, S. Tezer, Process Biochem. 40 (2005) 1347–1361.
[24] Z.D. Wei, R. Wang, Chin. Chem. Lett. 27 (2016) 769–772.
[25] H. Yao, X.M. You, Q. Lin, et al., Chin. Chem. Lett. 24 (2013) 703–706.
[26] T. Xue, B. Peng, M. Xue, et al., Nat. Commun. 5 (2014) 3200.
[27] J.T. Hupp, Nat. Chem. 2 (2010) 432–433.
[28] T.C. Bruice, Acc. Chem. Res. 24 (1991) 243–249.
[29] M. Liu, H. Zhao, S. Chen, et al., ACS Nano 6 (2012) 3142–3151.
[30] J. Gao, F. Liu, Y.L. Liu, et al., Chem. Mat. 22 (2010) 2213–2218.
[31] L.G.M.J. Ferna'ndez-Merino, J.I. Paredes, S. Villar-Rodil, et al., J. Mater. Phy. Chem. C 114 (2010) 6426–6432.
[32] J. Bredenbeck, J. Helbing, K. Nienhaus, et al., P. Natl. Acad. Sci. U. S. A. 104 (2007) 14243–14248.
[33] C. Walling, Acc. Chem. Res. 8 (1975) 125–131.
[34] K. Ishibashi, A. Fujishima, T. Watanabe, K. Hashimoto, Electrochem. Commun. 2 (2000) 207–210.
[35] X. Hai, Z. Guo, X. Lin, et al., ACS Appl. Mater. Interfaces 10 (2018) 5853–5861.
[36] Y.Y. Yao, Y.J. Mao, Q.F. Huang, et al., J. Hazard. Mater. 264 (2014) 323–331.
[37] X.J. Yang, X.M. Xu, J. Xu, Y.F. Han, J. Am. Chem. Soc. 135 (2013) 16058–16061.
[38] D. Lv, R. Wang, G. Tang, Z. Mou, et al., ACS Appl. Mater. Interfaces 11 (2019) 12880–12889.
[39] G.K. Ramesha, A.V. Kumara, H.B. Muralidhara, S. Sampath, J. Colloid. Interface Sci. 361 (2011) 270–277.
[40] Z. Ma, Y. Qiu, H. Yang, et al., Appl. Mater. Interfaces 7 (2015) 22036–22045.
[41] M. Garcia-Viloca, J. Gao, M. Karplus, D.G. Truhlar, Science 303 (2004) 186–195.